Intracellular Phospholipase A₁γ (iPLA₁γ) Is a Novel Factor Involved in Coat Protein Complex I- and Rab6-independent Retrograde Transport between the Endoplasmic Reticulum and the Golgi Complex*▣

Rei K. Morikawa[‡1], **Junken Aoki**[‡§¶2], **Fumi Kano**[∥], **Masayuki Murata**[∥], **Akitsugu Yamamoto**[**], **Masafumi Tsujimoto**[‡‡], **and Hiroyuki Arai**[‡§§]

*From the ‡Graduate School of Pharmaceutical Sciences, The University of Tokyo, 7-3-1 Hongo, Bunkyo-ku, Tokyo 113-0033, §Graduate School of Pharmaceutical Sciences, Tohoku University, 6-3 Aobayama, Aoba-ku, Sendai 980-8578, ∥Department of Life Sciences, Graduate School of Arts and Sciences, The University of Tokyo, 3-8-1 Komaba, Meguro-ku, Tokyo 153-8902, **Department of Bio-Science, Nagahama Institute of Bio-Science and Technology, Nagahama 526-0829, ‡‡Laboratory of Cellular Biochemistry, RIKEN, 2-1 Hirosawa, Wako, Saitama 351-0198, and ¶PRESTO and §§CREST, Japan Science and Technology Agency, 4-1-8 Honcho, Kawaguchi, Saitama 332-0012, Japan*

The mammalian intracellular phospholipase A₁ (iPLA₁) family consists of three members, iPLA₁α/PA-PLA₁, iPLA₁β/p125, and iPLA₁γ/KIAA0725p. Although iPLA₁β has been implicated in organization of the ER-Golgi compartments, little is known about the physiological role of its closest paralog, iPLA₁γ. Here we show that iPLA₁γ mediates a specific retrograde membrane transport pathway between the endoplasmic reticulum (ER) and the Golgi complex. iPLA₁γ appeared to be localized to the cytosol, the *cis*-Golgi, and the ER-Golgi intermediate compartment (ERGIC). Time-lapse microscopy revealed that a population of GFP-iPLA₁γ was associated with transport carriers moving out from the Golgi complex. Knockdown of iPLA₁γ expression by RNAi did not affect the anterograde transport of VSVGts045 but dramatically delayed two types of Golgi-to-ER retrograde membrane transport; that is, transfer of the Golgi membrane into the ER in the presence of brefeldin A and delivery of cholera toxin B subunit from the Golgi complex to the ER. Notably, knockdown of iPLA₁γ did not impair COPI- and Rab6-dependent retrograde transports represented by ERGIC-53 recycling and ER delivery of Shiga toxin, respectively. Thus, iPLA₁γ is a novel membrane transport factor that contributes to a specific Golgi-to-ER retrograde pathway distinct from presently characterized COPI- and Rab6-dependent pathways.

Phospholipase A₁ (PLA₁)[3] is an enzyme that hydrolyzes an acyl group from phospholipids at the *sn*-1 position. Although

PLA₁ activity had been detected widely in many cells and tissues, its physiological function and the molecules responsible for this enzymatic activity had been unclear for a long time (1, 2). In the late 1990s, the first intracellular PLA₁ was purified and cloned from bovine testis. It exhibited PLA₁ activity toward phosphatidic acid (PA) and was named PA-preferring PLA₁ (PA-PLA₁) (3–5). Similar PLA₁ activity was observed in brain and testis by two other independent groups (6, 7). From the study of Uchiyama *et al.* (7), it is likely that PA-PLA₁ exhibits PLA₁ activity toward not only PA but also other phospholipids depending on the assay conditions employed. Molecular cloning of PA-PLA₁ revealed that intracellular PLA₁ (iPLA₁) forms a protein family well conserved throughout eukaryotes (5, 8, 9), suggesting their fundamental roles in eukaryotic cells. However, their physiological substrates as well as their functions are not well understood.

Mammals have three intracellular PLA₁ homologs: PA-PLA₁, p125, and KIAA0725p. p125 was originally identified in a search for a new membrane transport factor that interacts with Sec23p (10). KIAA0725p was afterward identified as a close paralog of p125 by a database search (11). Because these proteins were identified in different studies with different strategies, they were named based on discrete properties such as *in vitro* substrate, the molecular size, and the gene number in the cDNA screening project. For clarification, we propose here a unified nomenclature for these mammalian iPLA₁s (PA-PLA₁ as iPLA₁α, p125 as iPLA₁β, and KIAA0725p as iPLA₁γ), according to the order of their identification. Hereafter we adopt this new nomenclature.

In addition to the three mammalian iPLA₁s, iPLA₁ genes are found in various eukaryotic model organisms. Studies of these homologs suggest that iPLA₁ family proteins contribute to diverse biological processes but are generally regulators of

---

[1] Present address: Center for Frontier Research, National institute of Genetics, 1111 Yata, Mishima, Shizuoka 411-8584, Japan.
[2] To whom correspondence should be addressed: Graduate School of Pharmaceutical Sciences, Tohoku University, 6-3 Aobayama, Aoba-ku, Sendai 980-8578, Japan. Tel.: 81-22-795-6860; Fax: 81-22-795-6859; E-mail: jaoki@mail.pharm.tohoku.ac.jp.
[3] The abbreviations used are: PLA₁, phospholipase A₁; iPLA₁, intracellular PLA₁; PLA₂, phospholipase A₂; ER, endoplasmic reticulum; ERGIC, ER-Golgi intermediate compartment; COPI, coat protein complex I; COPII, coat pro-

tein complex II; VSVG, vesicular stomatitis virus glycoprotein; GT, galactosyltransferase; GFP, green fluorescent protein; CtxB, cholera toxin B subunit; Stx, Shiga toxin; BFA, brefeldin A; PA, phosphatidic acid; FRAP, fluorescence recovery after photobleaching; siRNA, small interfering RNA; CHO, Chinese hamster ovary; Pipes, 1,4-piperazinediethanesulfonic acid; PBS, phosphate-buffered saline.

membrane dynamics. For example, SGR2, an iPLA$_1$ homolog in *Arabidopsis thaliana*, was reported to be involved in plant shoot gravitropism probably through regulating vacuolar membrane dynamics in gravity-sensing cells (9). ipla-1 of *Caenorhabditis elegans* regulates stem cell division and genetically interacts with genes involved in endosome-to-Golgi membrane transport (8). Mammalian iPLA$_1\beta$ has been implicated in the ER-Golgi organization as shown by the following. 1) iPLA$_1\beta$ physically interacts with Sec23p, a component of COPII complex that plays a crucial role in vesicle formation at the ER exit sites and is also localized to these compartments. 2) Overexpression of iPLA$_1\beta$ disrupts the structures of the Golgi complex and the ERGIC. 3) Knockdown of iPLA$_1\beta$ by RNAi causes changes in distribution of the ER exit sites (10, 12).

iPLA$_1\gamma$ is the closest paralog of iPLA$_1\beta$ (40.3% amino acid sequence homology). Because iPLA$_1\gamma$ shows high homology to iPLA$_1\beta$ and because overexpression of iPLA$_1\gamma$, like overexpression of iPLA$_1\beta$, leads to disorganization of ER-Golgi compartments (11), iPLA$_1\beta$ and -γ appear to play similar roles in ER-Golgi membrane transport or maintenance. However, it should be noted that iPLA$_1\gamma$ does not interact with Sec23p, to which iPLA$_1\beta$ binds (11). In addition, iPLA$_1\gamma$ exhibits extensive PLA$_1$ activity toward various phospholipids *in vitro* (10, 11, 13), whereas iPLA$_1\beta$ has not yet been shown any detectable PLA$_1$ activity. Thus, the physiological role of iPLA$_1\gamma$ has remained obscure.

Phospholipid is a major constituent of biomembranes, and phospholipid and its metabolism have been proposed to play important roles in regulation of membrane dynamics (14–20). Particularly, Brown and co-workers (21–24) have shown using phospholipid metabolism inhibitors that specific phospholipid metabolisms are involved in the ER-Golgi membrane transport. For example, phospholipase A$_2$ (PLA$_2$) inhibitors such as ONO-RS-082 and BEL blocked the constitutive Golgi-to-ER retrograde transport. CI-976, an inhibitor of lysophospholipid acyltransferase, caused Golgi membrane tubulation and transfer into the ER. These studies predicted that phospholipid deacylation promotes and, conversely, reacylation inhibits retrograde transport between the ER and the Golgi complex. However, the enzyme responsible for these phenomena has not been identified. It does not appear to be cytosolic or intracellular PLA$_2$ because cytosolic and intracellular PLA$_2$ knock-out mice are viable and grow normally. It must be also noted that the inhibitors used in the experiments above affect a broad range of phospholipases or acyltransferases. Thus, it is possible that PLA$_1$ contributes to the Golgi-to-ER retrograde transport.

The presently best characterized Golgi-to-ER pathways involve the COPI complex and Rab6. COPI is a coatomer complex that mediates vesicle formation at the ERGIC/*cis*-Golgi compartments. COPI-coated vesicles retrieve ER-resident proteins with specific signals (KK*XX* for membrane proteins and KDEL for luminal proteins) from the post-ER compartments and carry them back to the ER (25, 26). Rab6 is a small G protein localized to the Golgi membranes and has recently been shown to mediate COPI-independent Golgi-to-ER transport of a Golgi-resident enzyme and a protein toxin, Shiga toxin (Stx) (27, 28). Other Golgi-to-ER retrograde pathways have been also suggested (29), although their components are unknown.

In this study we demonstrate that iPLA$_1\gamma$ is localized to the *cis*-Golgi and ERGIC and involved in Golgi-to-ER retrograde transport. Moreover, we show that this pathway is distinct from the previously characterized COPI- and Rab6-dependent pathways. Our results provide not only new information on iPLA$_1$ family but also insights into a novel retrograde transport pathway regulated by a newly emerging lipid-metabolizing enzyme.

EXPERIMENTAL PROCEDURES

Antibodies and Reagents—Anti-iPLA$_1\gamma$ rat monoclonal antibodies (3G1 and 8F12) were generated as follows. Briefly, a polypeptide (amino acid number 368–486 of human iPLA$_1\gamma$) was expressed as a glutathione *S*-transferase fusion protein in *Escherichia coli*, and the purified protein was used to immunize rats (WKY/Izm). The medial iliac lymph nodes from the rats were used for cell fusion with mouse myeloma cells, PAI. Two hybridoma clones were established, 3G1 and 8F12. 3G1 recognized human and mouse iPLA$_1\gamma$ in Western blotting. 8F12 was reactive to human, mouse, and Chinese hamster iPLA$_1\gamma$ in both Western blotting and immunocytochemistry. The following antibodies were also used: mouse anti-GS28 and anti-GM130 monoclonal antibodies (BD Transduction Laboratories), mouse anti-β-COP antibody maD (Sigma), mouse anti-ERGIC-53 monoclonal antibody (kindly donated by Dr. H. P. Hauri, University of Basel, Switzerland), anti-GFP antibody (kindly provided by Dr. N. Nakamura, Kanazawa University, Japan), mouse anti-α-tubulin monoclonal antibody DM1A (Sigma). Stx and rabbit anti-Stx polyclonal antibody were kindly donated by Dr. K. Nishikawa and Dr. Y. Natori (International Medical Center of Japan). All fluorescent Alexa-labeled secondary antibodies and Alexa 594-conjugated cholera toxin B subunit (CtxB) were obtained from Molecular Probes. Horseradish peroxidase-labeled secondary antibodies were obtained from either GE Healthcare or American Qualex. Brefeldin A and Geneticin were obtained from Sigma and Invitrogen.

Fluorescent Protein Fusion Constructs—cDNAs encoding human iPLA$_1\gamma$ and human ϵCOP were cloned into pEGFP-C3 vector (Clontech) to generate GFP-iPLA$_1\gamma$ and GFP-ϵCOP. cDNA encoding amino acids 1–60 of mouse GT was cloned into pEGFP-N1 vector to generate GFP-tagged galactosyltransferase (GT-GFP). To generate GFP-ERGIC-53, pssGFP vector was first established by inserting the signal sequence of Chinese hamster ERGIC-53 (p58) in front of the cDNA for EGFP in pEGFP-C1. The cDNA encoding Chinese hamster ERGIC-53 lacking the signal sequence was then inserted into the multicloning site of pssGFP vector. The cDNA encoding GFP-tagged ts045 vesicular stomatitis virus protein (VSVGts045-GFP) was a gift from Dr. J. Lippincott-Schwartz (National Institutes of Health).

Cell Culture, Transfection, and Establishment of GFP-iPLA$_1\gamma$ Stably Expressing Cells—HeLa cells were grown in Dulbecco's modified Eagle's medium containing 10% fetal bovine serum, 100 units/ml penicillin, and 100 μg/ml streptomycin. Stably transfected CHO cells were cultured in Ham's F-12 medium containing 10% fetal bovine serum, 100 units/ml penicillin, 100 μg/ml streptomycin, and 300 μg/ml Geneticin. Cells at subconfluency were transfected with plasmids carrying the indicated cDNAs using FuGENE 6 (Roche Diagnostics) or Lipofectamine

2000 (Invitrogen) according to the manufacturer's instructions. For iPLA$_1\gamma$ knockdown experiments, HeLa cells at subconfluency were transfected with siRNA against iPLA$_1\gamma$ mRNA (GGAUGAGUAUGGACCUUAAGAACAA) and either scrambled siRNA (UGGAUAUGUACACAAGAGAUAG-GAC) or *Silencer*^{TM} Negative Control #1 siRNA (Ambion) as a control using Lipofectamine 2000. The day after, transfection cells were passaged to fresh dishes and allowed to grow for another 48 h before experiments were started. To establish GFP-iPLA$_1\gamma$ stably expressing CHO cells, GFP-iPLA$_1\gamma$ was transfected to CHO cells, and stably expressing cells were selected in complete medium containing 300 μg/ml Geneticin.

Immunofluorescence and Time-lapse Microscopy—For immunofluorescent staining, cells were grown on either 35-mm glass-bottomed dishes (Iwaki) or glass coverslips and fixed with 3% paraformaldehyde in 100 mM Pipes-KOH, pH 7.2, 3.6 mM CaCl$_2$, 2 mM MgCl$_2$ for 30 min. After permeabilization with 0.5% Triton X-100 in PBS, cells were blocked in 3% bovine serum albumin-containing PBS for 1 h. After blocking, cells were incubated with primary antibodies for 2 h and subsequently with fluorescence-labeled secondary antibodies for 1 h. The samples were observed with a confocal microscope, LSM510 (Carl Zeiss).

Time-lapse imaging was also performed with the same confocal microscope system. Sequential images were acquired every 3 s by scanning the specimen with a low powered laser (3%) at room temperature.

Immunoelectron Microscopy—Cells cultured on plastic coverslips (Celldesk LF1, Sumitomo Bakelite) were fixed with 4% paraformaldehyde in PBS for 2 h and then subjected to the pre-embedded gold enhancement immunogold method using an anti-GFP antibody as previously described (30). Ultra-thin sections were prepared and observed with H-7600 (Hitachi).

VSVG Transport Assay—Cells were transfected with VSVGts045-GFP followed by incubation at 39 °C for 16 h to allow VSVGts045 to accumulate in the ER. Then the cells were transferred to 32 °C to start the transport of VSVGts045. After incubation for various times, cells were fixed with 3% paraformaldehyde for 30 min and examined by confocal microscopy. Quantitative analysis was carried out by counting cells in which VSVGts045-GFP was localized at the ER, the Golgi complex, or the plasma membrane. Localization of VSVGts045-GFP at the ER and the Golgi complex was judged by its nuclear ring plus a network pattern typical for the ER and stacked Golgi pattern at the perinuclear region.

CtxB and Stx Transport Assay—CtxB and Stx transport assays were performed with essentially the same procedure. Cells were incubated in medium containing Alexa 594-conjugated CtxB or non-labeled Stx on ice for 30 min to bind the toxins to the cell surface. After extensive washing with PBS to remove the unbound toxins, the cells were incubated in normal medium at 37 °C to allow the toxins to transport from the plasma membrane to the ER via the Golgi complex. After incubation for various time periods, the cells were fixed with 3% paraformaldehyde for 30 min, and then the localization of the toxins were examined. Alexa 594 conjugated to CtxB was detectable by confocal microscopy after fixation. Stx taken up by the cells was immunostained using an anti-Stx antibody to

visualize its localization. For examining localization of the toxins at the Golgi complex, the cells were co-stained with an anti-GM130 antibody as a Golgi marker. Localization of the toxins at ER was judged by the appearance of the nuclear ring pattern.

Induction of the Golgi Membrane Transfer to the ER by Brefeldin A (BFA) Treatment—The Golgi membrane was visualized by transfecting cDNA for GT-GFP. GT-GFP-transfected cells were treated with 10 μg/ml BFA for the indicated times and fixed with 3% paraformaldehyde for 30 min. The cells were observed under confocal microscopy. For morphometric analysis, the appearance of the Golgi membrane was classified into four stages: (*a*) Golgi, (*b*) Golgi + tubules, (*c*) tubules + ER, and (*d*) ER. The percentages of the cells in each stage were quantified at each time point.

Fluorescence Recovery after Photobleaching (FRAP) Analysis—Cells expressing GFP-ϵCOP or GFP-ERGIC-53 were grown on 35-mm glass-based dishes (Iwaki) and set on a stage of a Zeiss LSM 510 confocal microscope. The Golgi area was repeatedly photobleached (50 scans) using an argon laser (488 nm) with 100% laser power. After bleaching, sequential images were acquired to monitor the fluorescence recovery by scanning with low laser power (1%). The fluorescence intensity of the bleached Golgi area was measured using the Zeiss software. The resulting fluorescence recovery rates of ERGIC-53 and ϵCOP represent the recycling speed between the Golgi and the ER/ERGIC and the recruiting speed between a membrane and cytosolic pool, respectively.

RESULTS

iPLA$_1\gamma$ Is Associated with the ERGIC/cis-Golgi Compartments—To define subcellular localization of iPLA$_1\gamma$, we first examined the biochemical distribution of iPLA$_1\gamma$ in fractionated HeLa cell lysates. 70–80% of the total iPLA$_1\gamma$ was in the soluble fraction, and the rest was in the detergent-soluble membrane fraction (Fig. 1*A*). Because iPLA$_1$ family proteins lack a signal sequence at the N terminus, iPLA$_1\gamma$ is deduced to be a cytosolic and peripheral membrane protein. The localization of iPLA$_1\gamma$ was further analyzed by immunofluorescence microscopy. iPLA$_1\gamma$ appeared to be localized mainly to the cytosol and the Golgi complex, which was confirmed by colocalization with a Golgi marker GS28 (Fig. 1*B*, *top*). To examine the cellular localization of iPLA$_1\gamma$ in living cells, we established a CHO cell line stably expressing GFP-tagged iPLA$_1\gamma$ (CHO-GFP-iPLA$_1\gamma$). In these cells the protein expression level of GFP-iPLA$_1\gamma$ was more than 30-fold that of the endogenous iPLA$_1\gamma$ level of wild-type CHO cells (supplemental Fig. S1). However, the Golgi complex and the ERGIC were not perturbed in these cells as revealed by immunofluorescence of GM130, GS28, and ERGIC-53 (supplemental Fig. S2). In addition, distribution patterns of ER-Golgi membrane transport factors such as β-COP, Rab6, and ERGIC-53 were not changed in these cells (supplemental Fig. S2). Thus, it seems that transport between the ER and the Golgi complex is intact in CHO-GFP-iPLA$_1\gamma$. Like the endogenous iPLA$_1\gamma$ in HeLa cells, GFP-iPLA$_1\gamma$ was localized to the Golgi complex and the cytosol in these cells (Fig. 1*B*, *bottom*). Notably, GFP-iPLA$_1\gamma$ was additionally found in punctate structures of various sizes (0.2–0.8 μm) that did not contain the Golgi marker GS28 (Fig.
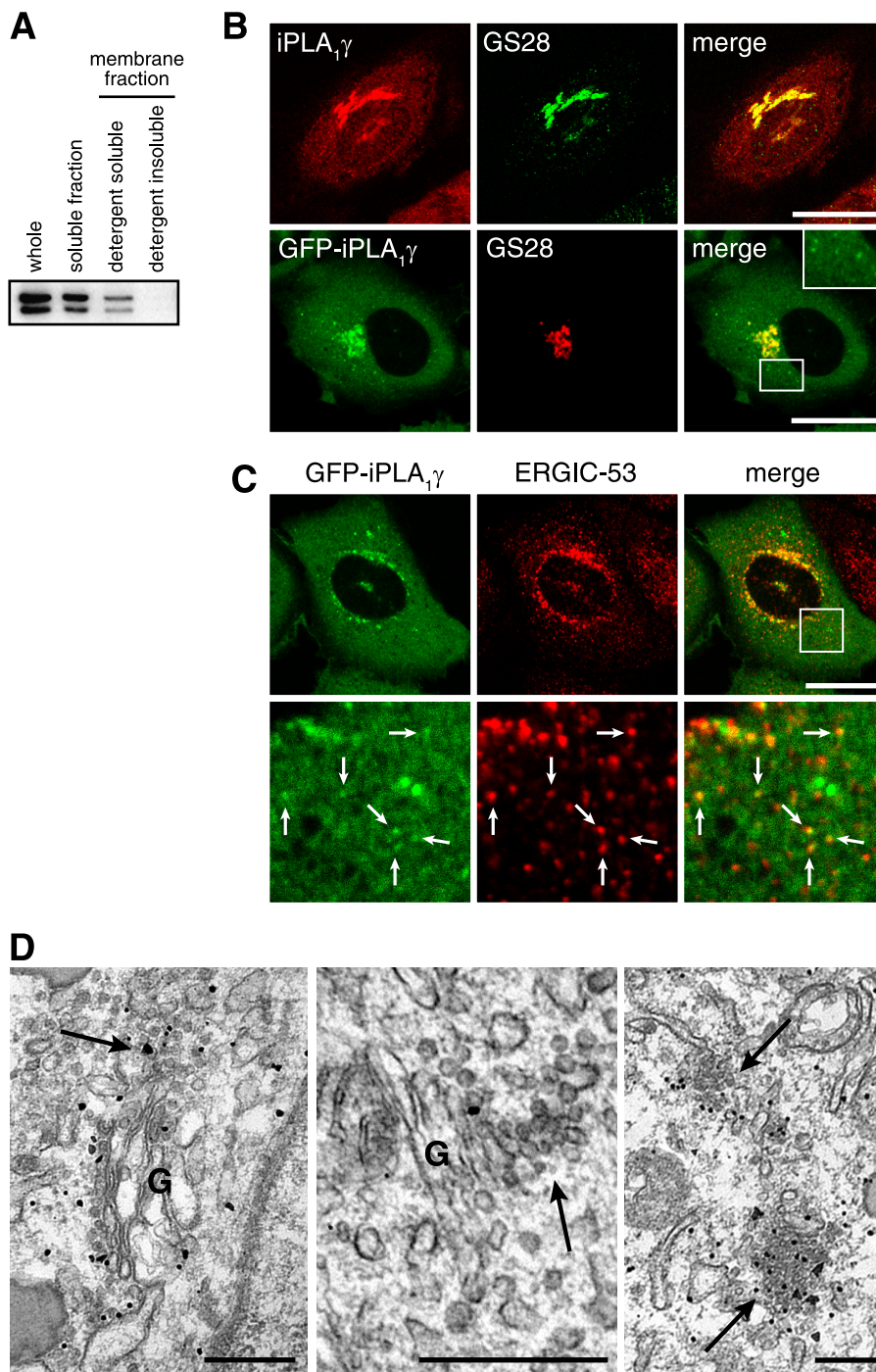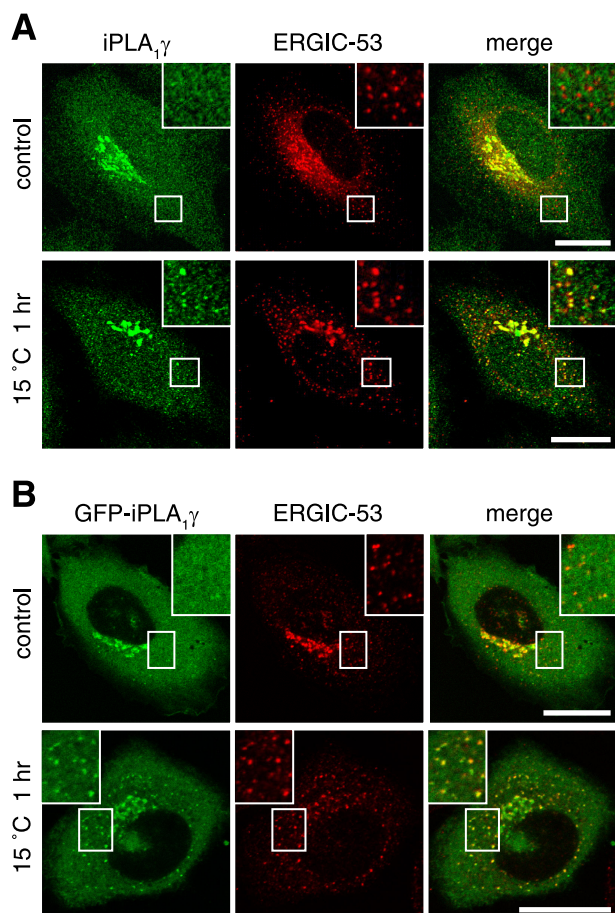
FIGURE 1. iPLA$_1\gamma$ is localized to the cytosol, the *cis*-Golgi, and the ERGIC. *A*, iPLA$_1\gamma$ distributes to both the cytosolic and the membrane fractions. Total homogenates of HeLa cells were fractionated into soluble, detergent-soluble, and detergent-insoluble fractions as described under "Experimental Procedures." Each fraction was subjected to Western blotting using anti-iPLA$_1\gamma$ antibody. *B*, localization of iPLA$_1\gamma$ under light microscopy. HeLa cells were fixed and double-stained with anti-iPLA$_1\gamma$ and anti-GS28 antibodies. iPLA$_1\gamma$ appeared to be localized to the cytosol and the Golgi complex (*top*). CHO-GFP-iPLA$_1\gamma$ cells were stained with an anti-GS28 antibody. GFP-iPLA$_1\gamma$ was localized not only to the Golgi complex and the cytosol but also to the dot-like structures (*bottom*). *Bars*, 20 μm. *C*, CHO-GFP-iPLA$_1\gamma$ cells were stained with an anti-ERGIC-53 antibody. The *bottom* images are higher magnification of the *boxed region* in the *top*. GFP-iPLA$_1\gamma$-positive small dots were partly colocalized with ERGIC-53. *Bar*, 20 μm. *D*, the localization of GFP-iPLA$_1\gamma$ stably expressed in CHO cells examined by silver/gold enhanced immunogold electron microscopy using an anti-GFP antibody. *G* indicates the Golgi complex. The gold particles showing the presence of GFP-iPLA$_1\gamma$ were detected on the *cis* side of the Golgi complex (*left* and *middle*) and the ERGIC, which is also known as vesicular tubular complex (*arrows*). The Golgi cisternae facing toward the vesicular tubular complex were identified as the *cis*-Golgi. High expression of GFP-iPLA$_1\gamma$ causes swelling of the Golgi stacks (*left*). *Bars*, 500 nm.

1*B*, *bottom inset*). To characterize these structures, CHO-GFP-iPLA$_1\gamma$ cells were stained with antibodies against four organelle markers; EEA1 for early endosomes, cation-dependent mannose 6-phosphate receptor for late endosomes/lysosomes, transferrin receptor for recycling endosomes, and ERGIC-53 for the ERGIC. Among these markers, ERGIC-53 overlapped with some of the GFP-iPLA$_1\gamma$-positive puncta (Fig. 1*C*).

To further determine the precise localization of iPLA$_1\gamma$, we performed electron microscopic analysis of CHO-GFP-iPLA$_1\gamma$ cells using an anti-GFP antibody. Consistent with the immunofluorescence observations, immunogold-labeled GFP-iPLA$_1\gamma$ was found both in the cytosol and on the Golgi membranes. In the Golgi complex, the signal was specifically concentrated on the *cis*-side (Fig. 1*D*, *left* and *middle*). The Golgi stacks with high expression of GFP-iPLA$_1\gamma$ were often swelled (Fig. 1*D*, *left*), probably reflecting the disorganizing effect of iPLA$_1\gamma$ overexpression. Strong signals were also detected at clusters of tubules and vesicles near the ER. These structures represent the ERGIC, which is also known as the vesicular tubular complex based on its appearance at the ultra-structural level (31–34). The ER tubules around these clusters, however, did not show significant positive signals (Fig. 1*D*, *right*), corroborating that iPLA$_1\gamma$ is associated with the ERGIC but not with the ER exit sites.

Although GFP-iPLA$_1\gamma$ was localized to the ERGIC, endogenous iPLA$_1\gamma$ did not appear to be distributed to the ERGIC in the immunofluorescence observations (Fig. 1*B*). To address the association of endogenous iPLA$_1\gamma$ with the ERGIC, we analyzed its localization at low temperature. At 15 °C, delivery of proteins from the ERGIC to the Golgi is blocked, resulting in accumulation of ER-Golgi recycling proteins in the ERGIC (33, 35). As shown in Fig. 2*A*, endogenous iPLA$_1\gamma$ showed marked colocalization with ERGIC-

A

B

FIGURE 2. **iPLA$_1$γ accumulates in the ERGIC at 15 °C.** *A*, HeLa cells were cultured at either 37 or 15 °C for 1 h followed by a double immunostaining with anti-iPLA$_1$γ and anti-ERGIC-53 antibodies. Endogenous iPLA$_1$γ did not appear to be localized to the ERGIC at 37 °C. At 15 °C, however, iPLA$_1$γ showed marked colocalization with ERGIC-53. *Bars*, 20 μm. *B*, GFP-iPLA$_1$γ stably expressed in CHO cells also showed colocalization with ERGIC-53 at 15 °C similarly to endogenous iPLA$_1$γ. *Bar*, 20 μm.

53 after 3 h of incubation at 15 °C, supporting the idea that endogenous iPLA$_1$γ associates with the ERGIC. A similar distribution pattern was observed for GFP-iPLA$_1$γ in CHO cells at 15 °C (Fig. 2*B*).

We next performed live imaging of GFP-iPLA$_1$γ using confocal microcopy. The GFP-iPLA$_1$γ localized to a Golgi region, punctate or globular structures (0.50 ± 0.13 μm) with low or little mobility, and highly mobile dot-like structures (0.35 ± 0.16 μm), which are likely transport carriers (Fig. 3*A* and a supplemental movie). It appears that some of these mobile structures have tubular protrusions that are small and very transient. Notably, we occasionally observed GFP-iPLA$_1$γ-positive structures (0.35 ± 0.05 μm) that arose from the Golgi region and traveled toward the cell periphery (Fig. 3*B* and a supplemental movie). Most of these structures disappeared in the peripheral region, possibly representing a release of iPLA$_1$γ from the membrane upon a fusion of the carrier with target organelles. These data suggest that iPLA$_1$γ is associated with not only the *cis*-Golgi and the ERGIC but also highly dynamic transport carriers.

iPLA$_1$γ Is Not Involved in the Anterograde Transport of VSVG but Contributes to the Retrograde Transport between the ER and

A

B
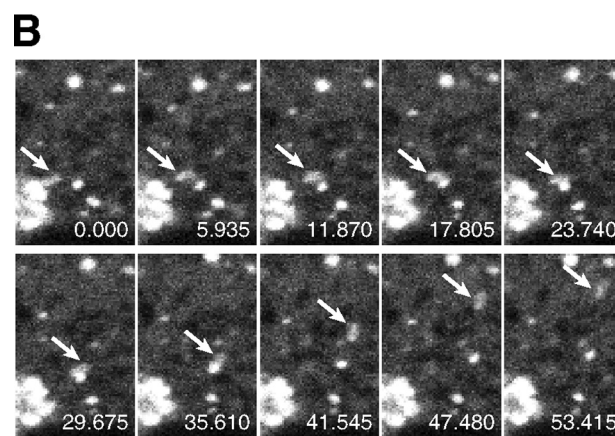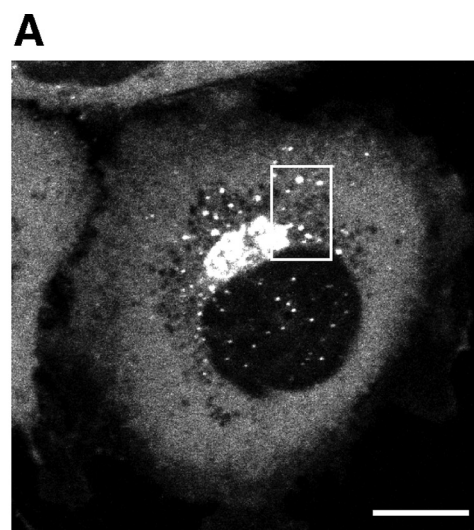
FIGURE 3. **GFP-iPLA$_1$γ is associated with transport carriers traveling from the Golgi complex to the cell periphery.** *A*, a CHO-GFP-iPLA$_1$γ cell observed under confocal microscopy. *Bar*, 10 μm. *B*, the time lapse images of the *boxed region* in *A*. Elapsed time in seconds is shown in each frame. A GFP positive structure arose from the Golgi complex and moved to the cell periphery (*arrow*) (see the supplemental movie).

the Golgi—Given the association of iPLA$_1$γ with the ERGIC and *cis*-Golgi, we tested whether iPLA$_1$γ plays a role in membrane transport between the ER and the Golgi complex by examining both anterograde and retrograde transports in iPLA$_1$γ-knockdown HeLa cells. Expression of iPLA$_1$γ was suppressed by transfecting the cells with siRNA against iPLA$_1$γ. The expression of iPLA$_1$γ protein was decreased to less than 10% that of control siRNA-treated cells as shown by Western blotting (Fig. 4*A*). The structures of the ER, the ER exit sites/ERGIC, and Golgi compartments were not obviously altered by iPLA$_1$γ knockdown as revealed by staining for organelle markers for these compartments (KDELR, ERGIC-53, and GM130, supplemental Fig. S3).

As a marker for anterograde transport, we used VSVGts045-GFP. VSVGts045 is a temperature-sensitive protein that accumulates in the ER at nonpermissive temperatures. Upon shifting to a permissive temperature, VSVGts045 starts to be transported along the secretory pathway via the Golgi complex (Fig. 4*B*), allowing the anterograde transport to be monitored (36, 37). iPLA$_1$γ knockdown cells showed a similar time course of VSVGts045-GFP transport from the ER to the Golgi complex

A

B

C
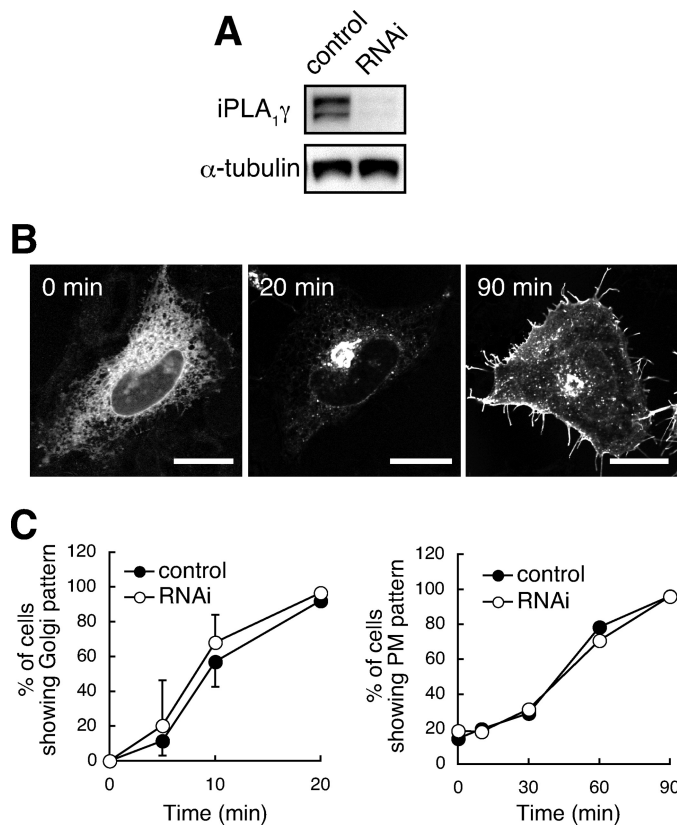
FIGURE 4. **Knockdown of iPLA$_1$γ does not affect the anterograde transport of VSVG.** *A*, HeLa cells were transfected with iPLA$_1$γ-specific or control siRNAs, and three days later expression of iPLA$_1$γ protein was examined by Western blotting with an anti-iPLA$_1$γ antibody. The protein level of iPLA$_1$γ was suppressed to less than 10% that in control cells by siRNA against iPLA$_1$γ. *B*, VSVG transport assay. In HeLa cells, VSVGts045-GFP accumulated in the ER at the restrictive temperature (39 °C). However, at the permissive temperature (32 °C), VSVGts045-GFP was rapidly transported to the Golgi complex and then to the plasma membrane along the secretory pathway. *Bars*, 20 μm. *C*, 2 days after siRNA transfection, the cells were retransfected with VSVGts045-GFP and cultured at 39 °C for 16 h. The cells were transferred to 32 °C to allow the transport of VSVGts045-GFP and fixed at various time points. The percentages of cells in which VSVGts045-GFP was localized at the Golgi complex (*left*) and the plasma membrane (*PM, right*) were quantified. For the *left graph*, data represent the mean ± S.D. (*n* = 2).

and plasma membrane to control cells (Fig. 4*C*), indicating that iPLA$_1$γ is not involved in the anterograde transport.

For analysis of the retrograde transport between the ER and the Golgi complex, we performed two assays. First we used BFA to induce Golgi membrane transfer into the ER. BFA is an inhibitor of guanine nucleotide exchanging factors of Arf and causes tubulation of the Golgi membrane and the following fusion of the tubules into the ER, resulting in redistribution of the Golgi membrane components into the ER (38–40). These Golgi membrane behaviors can be visualized by GT-GFP, a transmembrane Golgi-resident glycosylation enzyme (Fig. 5*A*) (41, 42). We introduced GT-GFP into control and iPLA$_1$γ knockdown cells and monitored the Golgi membrane behavior in the presence of BFA. In control cells GT-GFP was redistributed in the ER pattern by 30 min after the commencement of BFA treatment, indicating that most of the Golgi membrane was transferred to the ER within 30 min in these cells (Fig. 5*B, left*). In iPLA$_1$γ knockdown cells, however, GT-GFP-labeled tubules, which are intermediates of the membrane transport to

A

B

C
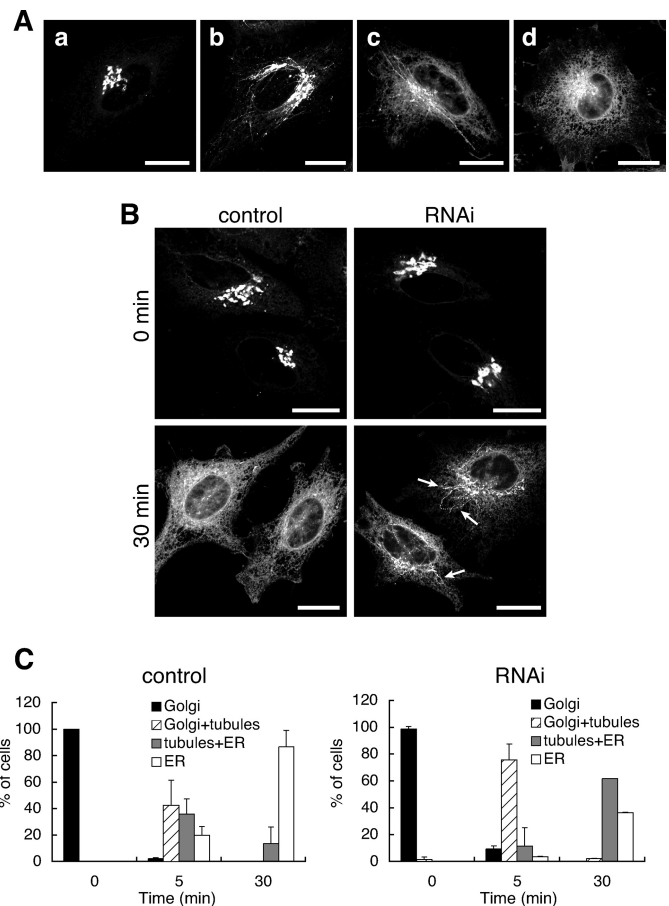
FIGURE 5. **Knockdown of iPLA$_1$γ causes a delay in BFA-induced Golgi membrane transfer to the ER.** *A*, the processes of the Golgi membrane transfer to the ER induced by BFA. The Golgi membrane was visualized by GT-GFP (*a–d*). *a* shows the Golgi structure in the steady state. The Golgi complex rapidly tubulates upon BFA treatment (*b*), and these tubules fuse with the ER, resulting in complete disappearance of the perinuclear Golgi structure (*c*). Eventually, all the Golgi membrane is redistributed in the ER, and GT-GFP exhibits the nuclear ring and network pattern, which is a typical appearance of the ER (*d*). *B*, two days after siRNA transfection, the cells were retransfected with GT-GFP. 20 h later, the cells were treated with 10 μg/ml BFA for indicated times and were fixed. The localization of GT-GFP was observed under confocal microscopy. After 30 min of BFA treatment, GT-GFP completely transferred to the ER in control cells. However, in iPLA$_1$γ knockdown cells, tubules containing GT-GFP (*arrows*) still remained after 30 min of BFA treatment. *Bars*, 20 μm. *C*, morphometric analysis of the Golgi membrane transport visualized by GT-GFP in control and iPLA$_1$γ knockdown cells in the presence of BFA. Control and iPLA$_1$γ knockdown cells expressing GT-GFP were treated with 10 μg/ml BFA for indicated times. The appearances of GT-GFP were classified into four stages as the typical images shown in *A*: Golgi (*a*), Golgi + tubules (*b*), tubules + ER (*c*), and ER (*d*). Data represent the mean ± S.D. (*n* = 2).

the ER, were frequently observed even after 30 min of BFA treatment (Fig. 5*B, right*). After 30 min of BFA treatment, 86.5% of the control cells showed GT-GFP redistributed throughout the ER, whereas 63.8% of the iPLA$_1$γ knockdown cells still retained GT-GFP-labeled tubular structures in the cytoplasm (Fig. 5*C*). These results demonstrate that iPLA$_1$γ knockdown caused a delay in Golgi membrane transport to the ER. It was also noted that in more than 90% of both control and iPLA$_1$γ knockdown cells the GT-GFP-labeled Golgi structures quickly collapsed and tubulated within 5 min (Fig. 5*C*). This suggests that this early step is normal in the iPLA$_1$γ knockdown cells and, therefore, that the subsequent steps, such as fusion of the tubules with the target membrane, were specifically impaired
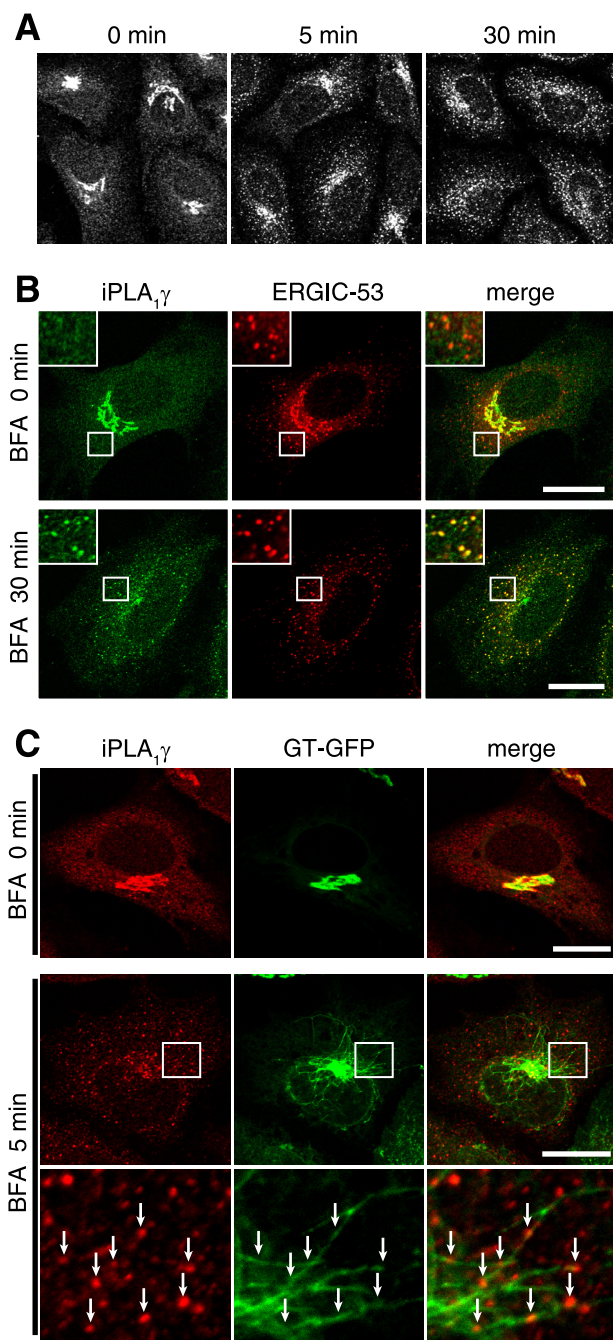
FIGURE 6. **iPLA$_1\gamma$ translocates from the Golgi complex to the ERGIC upon BFA treatment.** *A*, HeLa cells were treated with 10 μg/ml BFA for the indicated times and immunostained with an anti-iPLA$_1\gamma$ antibody. iPLA$_1\gamma$ showed a rapid translocation upon BFA treatment from the Golgi complex to dot-like structures dispersed throughout the cells. *Bar*, 50 μm. *B*, HeLa cells treated with 10 μg/ml BFA for 0 or 5 min were double-stained with anti-iPLA$_1\gamma$ and anti-ERGIC-53 antibodies. After 5 min of BFA treatment, iPLA$_1\gamma$ was colocalized with ERGIC-53 in the dot-like structures, indicating that iPLA$_1\gamma$ translocated from the Golgi complex to the ERGIC. *Bars*, 20 μm. *C*, HeLa cells were transfected with GT-GFP and treated with 10 μg/ml BFA for 0 or 5 min followed by immunostaining with an anti-iPLA$_1\gamma$ antibody. The iPLA$_1\gamma$-positive dots appeared to connect with the Golgi membrane tubules visualized by GT-GFP. *Bars*, 20 μm.

by iPLA$_1\gamma$ knockdown. After the addition of BFA, iPLA$_1\gamma$ translocated from the Golgi complex to punctate structures in the cell periphery, which is a typical distribution pattern for *cis*-Golgi resident proteins (Fig. 6*A*). These puncta were exten-
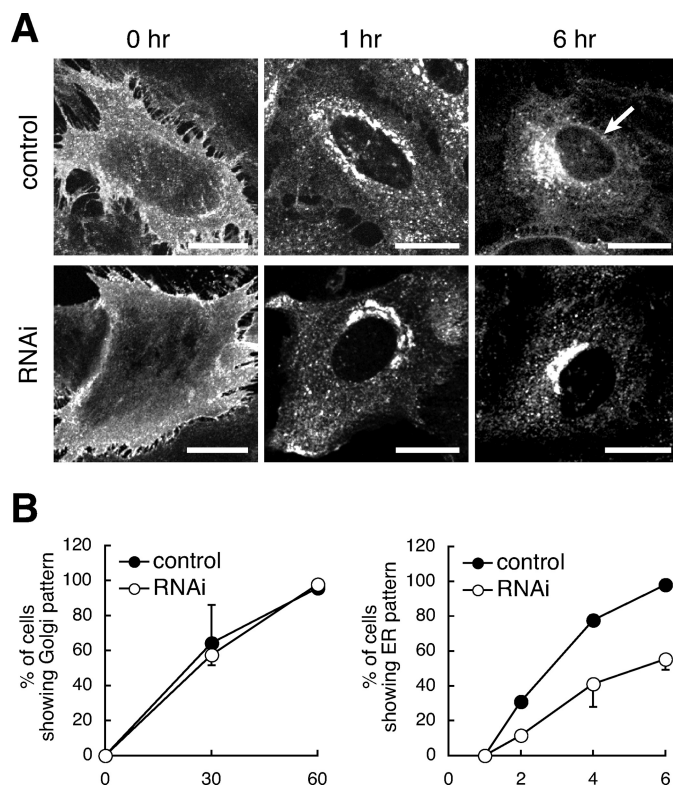
FIGURE 7. **Knockdown of iPLA$_1\gamma$ causes a delay in CtxB transport from the Golgi complex to the ER.** *A*, control and iPLA$_1\gamma$ knockdown cells were incubated with CtxB containing medium on ice for 30 min to allow CtxB to bind to the plasma membrane. After unbound CtxB was removed by washing with PBS, these cells were cultured in normal medium at 37 °C for indicated times and were then fixed. CtxB reached the Golgi complex at 1 h in both the control and iPLA$_1\gamma$ knockdown cells. CtxB reached the ER at 6 h in the control cell, which was confirmed by the nuclear ring pattern of CtxB (*arrow*). In contrast, in the iPLA$_1\gamma$ knockdown cell CtxB showed no nuclear ring pattern and mostly remained in the Golgi complex at 6 h. *Bars*, 20 μm. *B*, quantification of cells in which CtxB was localized to the Golgi complex (*left*) and the ER (*right*). iPLA$_1\gamma$ knockdown significantly delayed CtxB arrival in the ER. *Error bars* for control are hidden by the symbols. Data represent the mean $\pm$ S.D. ($n = 2$).

sively overlapped with the ERGIC spots stained with an anti-ERGIC-53 antibody (Fig. 6*B*), which have been thought to serve as an entrance for ER-destined carriers (43, 44). Double labeling of iPLA$_1\gamma$ and the Golgi membrane with an anti-iPLA$_1\gamma$ antibody and GT-GFP revealed that these iPLA$_1\gamma$-containing puncta were also overlapped with the Golgi membrane tubules in cells treated with BFA (Fig. 6*C*). These results show that iPLA$_1\gamma$ is present at the site of entrance of Golgi-derived tubular membranes into the ER.

Next, to analyze the retrograde transport without disturbing organelle integrity, we used CtxB as a transport marker in the second assay. Ctx is a protein toxin that invades cells by endocytosis and is further delivered to the ER via the *trans*-Golgi network (45, 46). It consists of an A subunit, which possesses toxic activity, and a B subunit, which binds to the cell surface receptor, a glycolipid GM1, and serves as a carrier for the A subunit to the ER. Thus, the B subunit, CtxB, can be used as a nontoxic retrograde transport marker. In both control and iPLA$_1\gamma$ knockdown cells, CtxB similarly bound to the plasma membrane during incubation on ice and reached the Golgi complex after 1 h of incubation at 37 °C (Fig. 7, *A* and *B*, *left*), indicating that endocytosis and the subsequent delivery to the
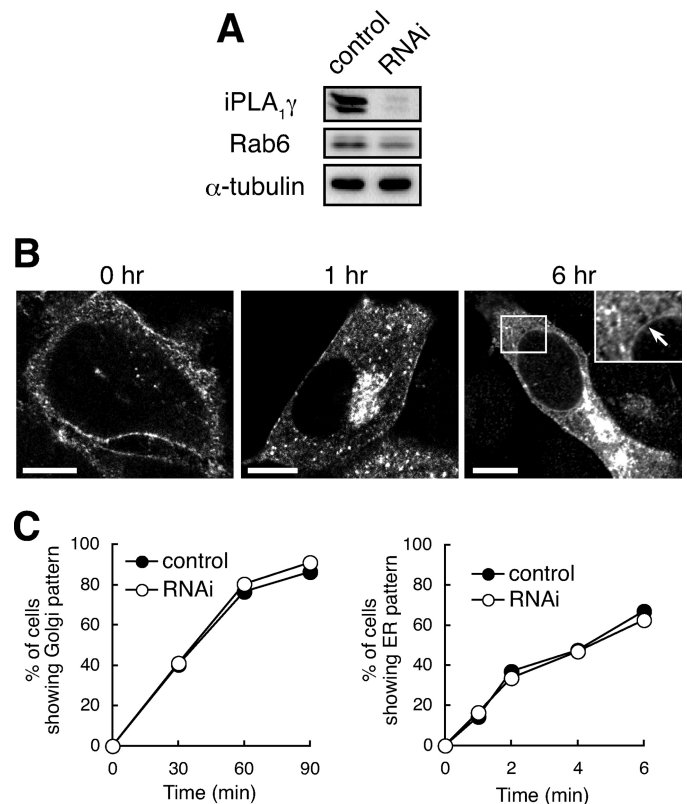
A
control | RNAi

B

C
control | RNAi

D
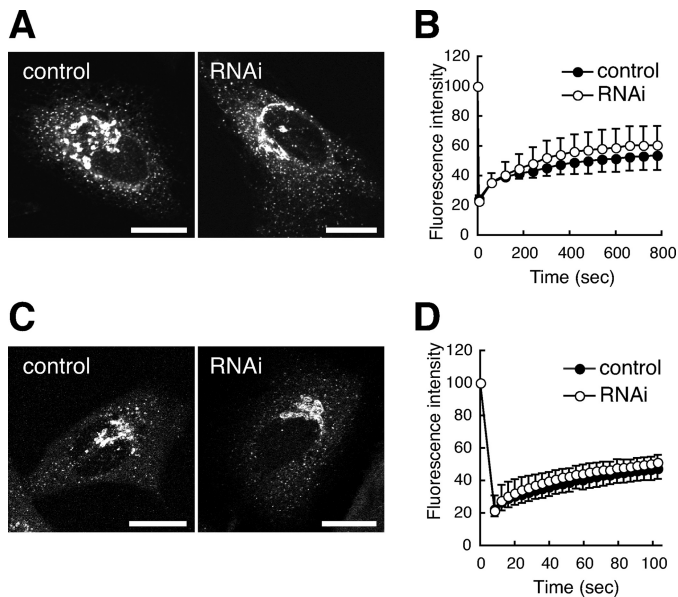
FIGURE 8. **Knockdown of iPLA₁γ does not affect the recycling speed of ERGIC-53 and the behavior of COPI complex.** *A*, control and iPLA₁γ knockdown HeLa cells expressing GFP-ERGIC-53. *Bars*, 20 μm. *B*, FRAP analysis of GFP-ERGIC-53. The Golgi regions were photobleached, and the fluorescence recovery was monitored. Data represent the mean ± S.D. (*n* = 3–4). *C*, control and iPLA₁γ knockdown HeLa cells expressing GFP-εCOP. *Bars*, 20 μm. *D*, FRAP analysis was performed as in *A* (*n* = 5).

A
control | RNAi
iPLA₁γ
Rab6
α-tubulin

B
0 hr | 1 hr | 6 hr

C

FIGURE 9. **Knockdown of iPLA₁γ does not affect the transport of Stx.** *A*, 3 days after siRNA transfection, expression level of each protein was examined by Western blotting. Rab6 protein was reduced in iPLA₁γ knockdown cells. *B*, the transport of Stx from the plasma membrane to the ER via the Golgi complex. Stx was bound to the surface of HeLa S3 cells on ice, and its transport was started by shifting the temperature to 37 °C. The cells were fixed after incubation for indicated times and immunostained with an anti-Stx antibody. Stx localized in the ER showed nuclear ring pattern (*arrow*). *Bars*, 10 μm. *C*, quantification of cells in which Stx localized to the Golgi complex (*left*) and the ER (*right*). At least two separate experiments were performed for both Golgi and ER arrivals of Stx, and typical results are presented here. The transport speed of Stx was not altered by iPLA₁γ knockdown.

Golgi complex were not affected in iPLA₁γ knockdown cells. On the other hand, the arrival of CtxB to the ER was remarkably delayed in iPLA₁γ knockdown cells. In control cells, CtxB reached the ER in 6 h, as judged by the nuclear ring pattern characteristic for the ER. In contrast, in more than 50% of the iPLA₁γ knockdown cells CtxB still remained in the Golgi complex and showed no ER-like pattern at 6 h (Fig. 7, *A* and *B*, *right*). Together, these results suggest that iPLA₁γ specifically contributes to Golgi-to-ER retrograde transport.

The Retrograde Pathway Involving iPLA₁γ Is Distinct from Both COPI- and Rab6-dependent Pathways—Given the involvement of iPLA₁γ in retrograde transport between the Golgi complex and the ER and the existence of multiple pathways from the Golgi complex to the ER, we next addressed in what pathway iPLA₁γ takes part. First, we examined whether iPLA₁γ knockdown affects COPI-dependent transport. One of the proteins that is transported via COPI is ERGIC-53, which is a cargo receptor for glycoproteins and constitutively cycles between the ER/ERGIC and the Golgi complex (31, 47). Using the FRAP technique against the Golgi region of GFP-ERGIC-53, we evaluated the transport speed of ERGIC-53 in control and iPLA₁γ knockdown HeLa cells. iPLA₁γ knockdown and control cells had similar distributions of GFP-ERGIC-53 (Fig. 8*A*), suggesting that the structures of the ER-Golgi compartments were not affected. FRAP analysis showed no significant difference in the time course of the fluorescence recovery between control and iPLA₁γ knockdown cells (Fig. 8*B*). These results suggest that iPLA₁γ is not involved in the cycling of ERGIC-53.

We also examined whether knockdown of iPLA₁γ alters the behavior of COPI itself. To visualize COPI, we expressed GFP-tagged εCOP (GFP-εCOP), a component of COPI, in HeLa cells

(48). COPI distributes to the ERGIC and the *cis*-Golgi, where it is recruited from the cytoplasm and functions as a coatomer to form vesicles. iPLA₁γ knockdown and control cells had similar distributions of GFP-εCOP (Fig. 8*C*). In addition, the fluorescence recovery rate of the Golgi region of GFP-εCOP in the FRAP analysis was not affected by iPLA₁γ knockdown (Fig. 8*D*), suggesting that the recruiting speed of GFP-εCOP was unaltered by iPLA₁γ knockdown. These results indicate that iPLA₁γ is not involved in the COPI-dependent retrograde pathway.

Another possible retrograde pathway in which iPLA₁γ is involved is the Rab6-dependent pathway (27, 28). In iPLA₁γ knockdown cells, the expression of Rab6 protein was reduced to 40–60% that of control (Fig. 9*A*). If this moderate reduction in Rab6 level is causative of the iPLA₁γ knockdown phenotype, Rab6-dependent pathway should be impaired in iPLA₁γ knockdown cells. To test this possibility, we performed Stx transport assay in iPLA₁γ knockdown cells. Stx is a protein toxin transported from the plasma membrane to the ER via the Golgi complex in a Rab6-dependent and COPI-independent manner (27, 49). In HeLa cells, Stx reaches the Golgi complex in 1 h and then reaches the ER in ~6 h (Fig. 9*B*). In iPLA₁γ knockdown cells, Stx was found to be transported in a similar time course to

control cells (Fig. 9*C*), indicating that knockdown of iPLA$_1\gamma$ does not functionally affect Rab6-dependent transport. Thus, it is likely that iPLA$_1\gamma$ does not directly participate in the Rab6-dependent pathway. Together, our results indicate that iPLA$_1\gamma$ is involved in a specific Golgi-to-ER retrograde transport pathway distinct from the previously characterized COPI- and Rab6-dependent pathways.

DISCUSSION

Transport Pathway and Processes Mediated by iPLA$_1\gamma$—Previous studies have suggested the existence of distinct Golgi-to-ER pathways other than the COPI- and Rab6-dependent pathways. However, very little is known about retrograde factors other than COPI and Rab6. In this study we have shown evidence suggesting that iPLA$_1\gamma$ contributes to a specific Golgi-to-ER retrograde transport distinct from the presently characterized COPI- and Rab6-dependent pathways.

Although knockdown of iPLA$_1\gamma$ did not affect the efficiency of Rab6-dependent transport of Stx, we detected an ~60% reduction of Rab6 protein in iPLA$_1\gamma$ knockdown cells. It has been reported that adequate suppression of Rab6 results in not only a delay in Stx transport but also structural defects of the Golgi complex such as compaction or disassembly (50, 51). However, we never found changes in structures of the ER-Golgi compartments in iPLA$_1\gamma$ knockdown cells. Therefore, it is assumed that the 60% reduction of Rab6 in iPLA$_1\gamma$ knockdown cells is not enough to cause defects and, rather, is a secondary effect of suppression of iPLA$_1\gamma$ functions.

We demonstrated that knockdown of iPLA$_1\gamma$ delayed ER delivery of CtxB. CtxB specifically binds to the glycosphingolipid GM1, which is concentrated in lipid rafts and is often used as a raft marker (45). Because the interaction between CtxB and GM1 is maintained throughout the transport from the plasma membrane to the ER (52), it is thought that CtxB follows the endogenous intracellular flow of lipid rafts. Recent studies using lipid binding toxins and lipid raft markers suggested that a retrograde pathway transports lipid raft components from the plasma membrane to the ER via the Golgi complex (45, 52, 53). However, little is known about the molecular machineries that regulate this pathway. It has been proposed that this pathway does not involve protein-based sorting but is solely dependent on lipid-based machinery (45). Based on our results, it is possible that iPLA$_1\gamma$ is one of the factors that contributes to this lipid-based transport in the Golgi-to-ER part.

iPLA$_1\gamma$ knockdown also delayed Golgi membrane transfer into the ER in the presence of BFA, as was observed in cells treated with PLA$_2$ inhibitors (22). Although it is unclear whether the tubule formation and their transport induced by BFA reflect the physiological retrograde membrane transport, our results provide some information about the transport process mediated by iPLA$_1\gamma$. iPLA$_1\gamma$ knockdown cells displayed Golgi membrane tubules still remaining in the cytoplasm after BFA treatment, whereas tubulation and collapse of the Golgi structure appeared normal in these cells. This suggests that iPLA$_1\gamma$ is not involved in the tubulation step but contributes to the later step, promoting the entrance of the membranes into the ER. Consistent with this idea, iPLA$_1\gamma$ was colocalized with Golgi membrane tubules at ERGIC spots, which are thought to be an entrance for ER-destined tubules or vesicles. Thus, it is conceivable that iPLA$_1\gamma$ directly regulates the entrance of carrier membranes at the ERGIC.

Under normal conditions iPLA$_1\gamma$ was associated with the *cis*-Golgi and the ERGIC. The ERGIC serves as an intermediate compartment between the ER and the Golgi complex, where cargos are sorted into both anterograde and retrograde transport pathways (31, 54). It is thought that the retrograde vesicles or tubules that have departed from the Golgi complex fuse with the ERGIC, and the cargos are then repackaged into newly formed carriers that subsequently travel to the ER. Considering the presence of iPLA$_1\gamma$ on transport carriers that emerged from the Golgi complex and the result that iPLA$_1\gamma$ knockdown inhibited not the tubulation step but the later step in Golgi membrane tubular transport in the presence of BFA, it is highly likely that iPLA$_1\gamma$ mediates the fusion step between the Golgi-derived retrograde carriers and the ERGIC membranes. At the sites of membrane fusion, both the carriers and the target membranes have to undergo dynamic changes. In such situations, iPLA$_1\gamma$ might contribute to modification of membranes possibly through phospholipid hydrolysis.

Possible Roles of Phospholipid Hydrolyzing Activity of iPLA$_1\gamma$—We recently showed that ipla-1, the sole iPLA$_1$ family protein in *C. elegans*, requires its catalytic activity to normally organize asymmetric cell division (8). Thus, it is likely that iPLA$_1\gamma$ also functions through phospholipid metabolizing. The key question here is how iPLA$_1\gamma$ regulates membrane transport events through its catalytic activity to hydrolyze phospholipid molecules. PLA$_1$ reaction produces saturated free fatty acids and unsaturated lysophospholipids. Because unsaturated lysophospholipids are much more hydrophilic than their precursor, diacyl phospholipids, they can be relatively easily released into the aqueous phase. We previously demonstrated that iPLA$_1\gamma$ *in vitro* hydrolyzes various phospholipids including phosphoinositides, which contribute to diverse cellular events including membrane transport. Thus, it is possible that iPLA$_1\gamma$ eliminates these functional phospholipids from membranes (13). Another prominent aspect of PLA$_1$ reactions is that their products, lysophospholipids, generally have an inverted cone shape with a bulky polar head and a smaller fatty acid moiety and, therefore, generate positive membrane curvature (55, 56). A number of studies have suggested that phospholipid hydrolysis induces morphological changes of membranes *in vitro* including fusion (57–59). However, it remains to be determined whether lipid-metabolizing enzymes have such roles *in vivo*. Based on our present study, iPLA$_1\gamma$ is a likely candidate for the lipid-metabolizing enzyme that regulates membrane shapes *in vivo*. Determining the physiological substrate of iPLA$_1\gamma$ would verify these possibilities and more clearly define the function of its phospholipid metabolism.

Differences between the Three Mammalian iPLA$_1$s—iPLA$_1\beta$ and -γ had been expected to have similar functions because 1) they showed high homology with each other, and 2) overexpression cause similar structural defects to the Golgi complex and the ERGIC (10, 11). However, our results strongly suggested that iPLA$_1\gamma$ has a distinct function from that of iPLA$_1\beta$. It has been reported that iPLA$_1\beta$ is localized specifically in the ER exit sites, and knockdown of iPLA$_1\beta$ leads to disorganiza-

tion of the ER exit sites (12). On the other hand, as we have shown in this study, iPLA$_1\gamma$ is associated with the ERGIC/*cis*-Golgi compartments but not with the ER exit sites. In addition, knockdown of iPLA$_1\gamma$ does not affect the apparent organization of the ER exit sites/ERGIC, corroborating its distinct localization and function. Whereas the middle and C-terminal regions of iPLA$_1\beta$ and -γ are highly homologous, their N-terminal regions show very low homology. iPLA$_1\beta$ interacts with Sec23p through this region, whereas iPLA$_1\gamma$ does not. This difference may be responsible for their distinct localization and, together with the difference in PLA$_1$ activity, contribute to their eventual functions.

The third mammalian iPLA$_1$, iPLA$_1\alpha$, shows less homology to iPLA$_1\beta$ and -γ (15.9% and 18.8%, respectively). It neither binds to Sec23p *in vitro* nor causes disorganization of the ER-Golgi compartments when overexpressed. Although little is known about the physiological function of iPLA$_1\alpha$, the *in vitro* substrate preference of iPLA$_1\alpha$ and its distribution between the soluble and the membrane fractions are similar to those of iPLA$_1\gamma$,[4] raising the possibility that iPLA$_1\alpha$ contributes to membrane transport in a similar manner to that of iPLA$_1\gamma$.

Conclusion—In this study we focused on one of the three mammalian iPLA$_1$s, iPLA$_1\gamma$, and found that iPLA$_1\gamma$ is localized to the *cis*-Golgi and the ERGIC and is involved in Golgi-to-ER retrograde membrane transport. Importantly, the iPLA$_1\gamma$-dependent pathway was distinct from the previously characterized COPI- and Rab6-dependent pathways. Further studies will establish the physiological substrate of iPLA$_1\gamma$, the functional mechanism of its enzymatic activity, and the precise processes mediated by iPLA$_1\gamma$.

REFERENCES

1. Inoue, A., and Aoki, J. (2006) *Future Lipidol.* **1,** 687–700
2. Inoue, K., Arai, H., and Aoki, J. (2004) *Phospholipase A1-Structures, Physiological, and Pathophysiological Roles in Mammals*, p. 23–29, Wiley-VCH Verlag GmbH, Weinheim, Germany
3. Higgs, H. N., and Glomset, J. A. (1994) *Proc. Natl. Acad. Sci. U.S.A.* **91,** 9574–9578
4. Higgs, H. N., and Glomset, J. A. (1996) *J. Biol. Chem.* **271,** 10874–10883
5. Higgs, H. N., Han, M. H., Johnson, G. E., and Glomset, J. A. (1998) *J. Biol. Chem.* **273,** 5468–5477
6. Pete, M. J., Ross, A. H., and Exton, J. H. (1994) *J. Biol. Chem.* **269,** 19494–19500
7. Uchiyama, S., Miyazaki, Y., Amakasu, Y., Kuwata, H., Nakatani, Y., Atsumi, G., Murakami, M., and Kudo, I. (1999) *J. Biochem.* **125,** 1001–1010
8. Kanamori, T., Inoue, T., Sakamoto, T., Gengyo-Ando, K., Tsujimoto, M., Mitani, S., Sawa, H., Aoki, J., and Arai, H. (2008) *EMBO J.* **27,** 1647–1657
9. Kato, T., Morita, M. T., Fukaki, H., Yamauchi, Y., Uehara, M., Niihama, M., and Tasaka, M. (2002) *Plant Cell* **14,** 33–46
10. Tani, K., Mizoguchi, T., Iwamatsu, A., Hatsuzawa, K., and Tagaya, M. (1999) *J. Biol. Chem.* **274,** 20505–20512
11. Nakajima, K., Sonoda, H., Mizoguchi, T., Aoki, J., Arai, H., Nagahama, M., Tagaya, M., and Tani, K. (2002) *J. Biol. Chem.* **277,** 11329–11335
12. Shimoi, W., Ezawa, I., Nakamoto, K., Uesaki, S., Gabreski, G., Aridor, M., Yamamoto, A., Nagahama, M., Tagaya, M., and Tani, K. (2005) *J. Biol. Chem.* **280,** 10141–10148
13. Morikawa, R., Tsujimoto, M., Arai, H., and Aoki, J. (2007) *Methods Enzymol.* **434,** 1–13
14. Bankaitis, V. A., Aitken, J. R., Cleves, A. E., and Dowhan, W. (1990) *Nature* **347,** 561–562
15. Emoto, K., and Umeda, M. (2000) *J. Cell Biol.* **149,** 1215–1224
16. Graham, T. R. (2004) *Trends Cell Biol.* **14,** 670–677
17. Schu, P. V., Takegawa, K., Fry, M. J., Stack, J. H., Waterfield, M. D., and Emr, S. D. (1993) *Science* **260,** 88–91
18. Yang, J. S., Gad, H., Lee, S. Y., Mironov, A., Zhang, L., Beznoussenko, G. V., Valente, C., Turacchio, G., Bonsra, A. N., Du, G., Baldanzi, G., Graziani, A., Bourgoin, S., Frohman, M. A., Luini, A., and Hsu, V. W. (2008) *Nat. Cell Biol.* **10,** 1146–1153
19. Pathre, P., Shome, K., Blumental-Perry, A., Bielli, A., Haney, C. J., Alber, S., Watkins, S. C., Romero, G., and Aridor, M. (2003) *EMBO J.* **22,** 4059–4069
20. Pfanner, N., Orci, L., Glick, B. S., Amherdt, M., Arden, S. R., Malhotra, V., and Rothman, J. E. (1989) *Cell* **59,** 95–102
21. Chambers, K., Judson, B., and Brown, W. J. (2005) *J. Cell Sci.* **118,** 3061–3071
22. de Figueiredo, P., Drecktrah, D., Katzenellenbogen, J. A., Strang, M., and Brown, W. J. (1998) *Proc. Natl. Acad. Sci. U.S.A.* **95,** 8642–8647
23. de Figueiredo, P., Drecktrah, D., Polizotto, R. S., Cole, N. B., Lippincott-Schwartz, J., and Brown, W. J. (2000) *Traffic* **1,** 504–511
24. Drecktrah, D., Chambers, K., Racoosin, E. L., Cluett, E. B., Gucwa, A., Jackson, B., and Brown, W. J. (2003) *Mol. Biol. Cell* **14,** 3459–3469
25. Lee, M. C., Miller, E. A., Goldberg, J., Orci, L., and Schekman, R. (2004) *Annu. Rev. Cell Dev. Biol.* **20,** 87–123
26. Sannerud, R., Saraste, J., and Goud, B. (2003) *Curr. Opin. Cell Biol.* **15,** 438–445
27. Girod, A., Storrie, B., Simpson, J. C., Johannes, L., Goud, B., Roberts, L. M., Lord, J. M., Nilsson, T., and Pepperkok, R. (1999) *Nat. Cell Biol.* **1,** 423–430
28. White, J., Johannes, L., Mallard, F., Girod, A., Grill, S., Reinsch, S., Keller, P., Tzschaschel, B., Echard, A., Goud, B., and Stelzer, E. H. (1999) *J. Cell Biol.* **147,** 743–760
29. Chen, A., AbuJarour, R. J., and Draper, R. K. (2003) *J. Cell Sci.* **116,** 3503–3510
30. Luo, H., Nakatsu, F., Furuno, A., Kato, H., Yamamoto, A., and Ohno, H. (2006) *Cell Struct. Funct.* **31,** 63–75
31. Appenzeller-Herzog, C., and Hauri, H. P. (2006) *J. Cell Sci.* **119,** 2173–2183
32. Bannykh, S. I., Rowe, T., and Balch, W. E. (1996) *J. Cell Biol.* **135,** 19–35
33. Klumperman, J., Schweizer, A., Clausen, H., Tang, B. L., Hong, W., Oorschot, V., and Hauri, H. P. (1998) *J. Cell Sci.* **111,** 3411–3425
34. Sesso, A., de Faria, F. P., Iwamura, E. S., and Correa, H. (1994) *J. Cell Sci.* **107,** 517–528
35. Saraste, J., and Kuismanen, E. (1984) *Cell* **38,** 535–549
36. Bergmann, J. E. (1989) *Methods Cell Biol.* **32,** 85–110
37. Presley, J. F., Cole, N. B., Schroer, T. A., Hirschberg, K., Zaal, K. J., and Lippincott-Schwartz, J. (1997) *Nature* **389,** 81–85
38. Casanova, J. E. (2007) *Traffic* **8,** 1476–1485
39. Klausner, R. D., Donaldson, J. G., and Lippincott-Schwartz, J. (1992) *J. Cell Biol.* **116,** 1071–1080
40. Lippincott-Schwartz, J., Yuan, L. C., Bonifacino, J. S., and Klausner, R. D. (1989) *Cell* **56,** 801–813
41. Kano, F., Sako, Y., Tagaya, M., Yanagida, T., and Murata, M. (2000) *Mol. Biol. Cell* **11,** 3073–3087
42. Sciaky, N., Presley, J., Smith, C., Zaal, K. J., Cole, N., Moreira, J. E., Terasaki, M., Siggia, E., and Lippincott-Schwartz, J. (1997) *J. Cell Biol.* **139,** 1137–1155
43. Lippincott-Schwartz, J., Donaldson, J. G., Schweizer, A., Berger, E. G., Hauri, H. P., Yuan, L. C., and Klausner, R. D. (1990) *Cell* **60,** 821–836
44. Mardones, G. A., Snyder, C. M., and Howell, K. E. (2006) *Mol. Biol. Cell* **17,** 525–538

[4] R. K. Morikawa, unpublished data.

45. Lencer, W. I., and Tsai, B. (2003) *Trends Biochem. Sci.* **28,** 639–645
46. Feng, Y., Jadhav, A. P., Rodighiero, C., Fujinaga, Y., Kirchhausen, T., and Lencer, W. I. (2004) *EMBO Rep.* **5,** 596–601
47. Hauri, H. P., Kappeler, F., Andersson, H., and Appenzeller, C. (2000) *J. Cell Sci.* **113,** 587–596
48. Presley, J. F., Ward, T. H., Pfeifer, A. C., Siggia, E. D., Phair, R. D., and Lippincott-Schwartz, J. (2002) *Nature* **417,** 187–193
49. Johannes, L., and Goud, B. (2000) *Traffic* **1,** 119–123
50. Young, J., Stauber, T., del Nery, E., Vernos, I., Pepperkok, R., and Nilsson, T. (2005) *Mol. Biol. Cell* **16,** 162–177
51. Del Nery, E., Miserey-Lenkei, S., Falguières, T., Nizak, C., Johannes, L., Perez, F., and Goud, B. (2006) *Traffic* **7,** 394–407
52. Fujinaga, Y., Wolf, A. A., Rodighiero, C., Wheeler, H., Tsai, B., Allen, L., Jobling, M. G., Rapoport, T., Holmes, R. K., and Lencer, W. I. (2003) *Mol. Biol. Cell* **14,** 4783–4793
53. Nichols, B. J., Kenworthy, A. K., Polishchuk, R. S., Lodge, R., Roberts, T. H., Hirschberg, K., Phair, R. D., and Lippincott-Schwartz, J. (2001) *J. Cell Biol.* **153,** 529–541
54. Ben-Tekaya, H., Miura, K., Pepperkok, R., and Hauri, H. P. (2005) *J. Cell Sci.* **118,** 357–367
55. Brown, W. J., Chambers, K., and Doody, A. (2003) *Traffic* **4,** 214–221
56. McMahon, H. T., and Gallop, J. L. (2005) *Nature* **438,** 590–596
57. Blackwood, R. A., Transue, A. T., Harsh, D. M., Brower, R. C., Zacharek, S. J., Smolen, J. E., and Hessler, R. J. (1996) *J. Leukocyte Biol.* **59,** 663–670
58. Basáñez, G., Ruiz-Argüello, M. B., Alonso, A., Goñi, F. M., Karlsson, G., and Edwards, K. (1997) *Biophys. J.* **72,** 2630–2637
59. Stieglitz, K. A., Seaton, B. A., and Roberts, M. F. (2001) *Biochemistry* **40,** 13954–13963